Calculation of the intrinsic solvation free energy profile of methane across a liquid/liquid interface in computer simulations

Mária Darvas,[1,*] Miguel Jorge[2], M. Natalia D. S. Cordeiro[3], Pál Jedlovszky[4,5,6]

[1]*SISSA, Sector of Molecular and Statistical Biophysics, 265 via Bonomea, 34136 Trieste, Italy*

[2]*Department of Chemical and Process Engineering, University of Strathclyde, 75 Montrose Street, Glasgow G1 1XJ, United Kingdom*

[3]*REQUIMTE, Faculdade de Ciências da Universidade do Porto, Rua do Campo Alegre, 687, 4169-007 Porto, Portugal*

[4]*Laboratory of Interfaces and Nanosize Systems, Institute of Chemistry, Eötvös Loránd University, Pázmány P. stny 1/A, H-1117 Budapest, Hungary*

[5]*MTA-BME Research Group of Technical Analytical Chemistry, Szt. Gellért tér 4, H-1111 Budapest, Hungary*

[6]*EKF Department of Chemistry, Leányka utca 6, H-3300 Eger, Hungary*

Running title: Intrinsic free energy profile of methane

[*]**Electronic mail:** mdarvas@sissa.it

Abstract:

The transfer of ions and neutral particles through water/organic interfaces has been widely studied in the last few decades by both experimental and theoretical methods. The reason for the never ceasing interest in this field is the importance of transport phenomena in electrochemistry, biochemistry and separation science. In the current paper the solvation Helmholtz free energy profile of a methane molecule is presented, with respect to the intrinsic (i.e., real, capillary wave corrugated) interface of water and 1,2-dichloroethane, as obtained from constrained molecular dynamics simulations. The results of the current calculation are analysed in comparison with the solvation free energy profile of the chloride ion across the same interface.

1. Introduction

The transport of ions and neutral penetrants across fluid interfaces (liquid-liquid, liquid-vapour interfaces or lipid membranes) are widely studied model cases of biologically important processes such as the transfer of drugs across the cell membrane [1-5]. The driving force and mechanism of these processes can be interpreted in the framework of statistical thermodynamics, supposing that the free energy profile of the transport phenomenon is known at reasonable resolution. Several experimental techniques, such as calorimetry, voltammetry, or their various combinations [6-10] are aimed at measuring the free energy difference between two states, e.g., a solvated and a non-solvated one, or two different solvated states. Nevertheless, the free energy profiles are only reproducible by the so-called single molecules optical tweezers experiments in special cases involving physico-chemical processes of biomacromolecules, such as DNA or RNA unwinding or protein folding [11].

In principle, computer simulation methods, such as molecular dynamics (MD) or Monte Carlo can be used to obtain the free energy profile along a carefully chosen reaction coordinate, since, in an ideal case, unbiased simulations can provide a set of sample configurations representing a given statistical mechanical ensemble. In the case of the canonical ensemble the $\rho(\xi)$ density profile of the microstates along the reaction coordinate ξ can be converted into the Helmholtz free energy profile, $A(\xi)$, according to the equation:

$$A(\xi) = -RT \ln \rho(\xi), \tag{1}$$

where R and T stand for the gas constant and absolute temperature, respectively. In practice, however, the microstates belonging to ξ values characterized by high potential energy are poorly represented in the sample due to the finite length of the simulation. This makes direct counting inaccurate in estimating the free energy of these states, including important features such as high energy transition states. This statistical unreliability calls for the use of enhanced sampling methods, developed to capture rare events, in which the system is restrained by a biasing potential to the reaction coordinate of interest. These methods include harmonic [12] and adaptive umbrella sampling [13], steered MD [14], metadynamics [15], potential of mean force (PMF) calculation by, e.g., the constrained MD algorithm [16,17], or the Widom test particle insertion method [18] and its cavity insertion variant [19]. For solvation free energy profile calculations across fluid interfaces,

these methods have been widely used for a number of non-ionic [19-28] and ionic penetrants [29-44] at various fluid interfaces.

The question of the sampling efficiency is not the only difficulty one has to face when calculating solvation free energy profiles across fluid interfaces in computer simulations. The other major problem comes from the fact that any fluid interface is corrugated, on the atomistic length scale, by dynamic fluctuations due to the presence of thermal capillary waves [45]. Substituting this capillary wave corrugated real surface (often referred to as the "intrinsic" surface of the given phase) by an ideally flat ("non-intrinsic") one, such as the Gibbs dividing surface, leads to a systematic error of unknown magnitude in calculating any interface-related property if the system is seen at atomistic resolution. This systematic error originates from the misidentification of a number of surface molecules as being in the bulk phase and *vice versa*. Further, the calculation of any profile along the macroscopic interface normal axis implies averaging the quantity of interest in slabs that are at a given distance from the interface. The error coming from the incorrect location of the interface along its macroscopic normal axis when it is estimated by a mathematical plane leads to incorrect distance values, and hence to a systematic error in the calculated profiles. Thus, for instance, it has been shown several times that the sigmoidal-like, non-intrinsic density profile of the molecules constituting a given phase turns into a profile exhibiting several minima and maxima (as akin to typical radial distribution functions) if the profile is calculated relative to the real, molecularly rough intrinsic surface rather than to an external coordinate [46-52]. Therefore, any physically meaningful calculation of the solvation free energy profile across fluid interfaces requires that it is determined *relative to this molecularly rugged surface* rather than to an external axis (or, equivalently, relative to an ideally flat planar surface), as it has been done in most studies.

In order to perform such calculations, one has to be able to reconstruct the exact position of the surface in every frame. This task is equivalent to identifying the full set of interfacial molecules for every saved configuration. The first attempt to perform such an analysis was made three decades ago by Stillinger, who stated that interfacial molecules differ from bulk phase ones in the sense that they are in direct contact with a percolating volume of empty space [53]. This approach, though theoretically correct, was never routinely used due to the enormous computational demand of its algorithm. More than 20 years later, Chacón and Tarazona developed their self-consistent Intrinsic Sampling Method, which attempts to find the covering surface that goes through at a set of pivot sites and the area of which is minimal [46]. Others tried to approximate the intrinsic interface by dividing the system into several slabs along the macroscopic surface normal axis, using a mesh with a resolution comparable with the capillary wave length, and defined the position of the interface in

each slab separately [22,31,54-58]. This method has been further elaborated by Jorge and Cordeiro, who proposed to use a considerably finer grid, and determined the number of slabs required for convergence [49]. Yet another method, called Identification of the Truly Interfacial Molecules (ITIM) has been developed recently by Pártay et al. [59]. In ITIM analysis a probe sphere of a given radius, R_p, is moved along test lines from the bulk opposite phase towards the surface of the phase to be analyzed. Once it touches the first molecule of the phase of interest, it is stopped, and the touched molecule is marked as being interfacial. The intrinsic surface itself is then approximated by the positions of the interfacial molecules. A completely different method, based on the relative distance between molecules of opposing phases has been proposed by Chowdhary and Ladanyi for liquid-liquid interfaces [48]. Finally, several intrinsic surface analysis methods that are free from the assumption that the interface itself is macroscopically planar, and thus more generally applicable, have been developed in the past few years [60-62]. A recent comparison of the various intrinsic surface determining techniques revealed that ITIM provides an excellent compromise between accuracy and computational cost [63].

Even with a relatively efficient interface analysis method at hand it is computationally demanding to perform an intrinsic analysis of the free energy profile of transfer, since the biased simulation itself requires greater computational resources than an unbiased one. In a previous paper [44] we have proposed a computationally feasible way of calculating the intrinsic solvation free energy profile of a single penetrant particle across fluid interfaces and applied it for the calculation of the intrinsic solvation free energy profile of a Cl^- ion across the water - 1,2-dichloroethane (DCE) liquid-liquid interface. In the current paper we report the analysis of the intrinsic solvation Helmholtz free energy profile of a neutral penetrant, namely methane, across the same liquid-liquid interface in comparison with the features of the ionic penetrant. As for the case of the chloride ion [44], we compute here the intrinsic methane free energy profile relative to the surface of the water phase.

The paper is organized as follows. In section 2 details of the computer simulations, intrinsic surface analysis and free energy calculations are given. In section 3, the intrinsic free energy profile is presented in comparison with the corresponding non-intrinsic profile, and compared also to the intrinsic solvation free energy profile of the Cl^- ion across the same interface. Finally, in section 4 the main conclusions of this study are summarised.

2. Computational details

2.1. Simulation of the interfacial system

Molecular dynamics simulations of the water-DCE liquid/liquid interfacial system containing one methane molecule at different, suitably chosen positions were performed on the canonical (*N*,*V*,*T*) ensemble at 298 K using the GROMACS 3.3.2 simulation program package [64]. The lengths of the *X*, *Y* and *Z* edges of the rectangular basic simulation box (*X* being perpendicular to the macroscopic plane of the interface) were 104, 50 and 50 Å, respectively. The system consisted of 4000 water, 1014 DCE, and one methane molecules.

The water molecules were described by the TIP4P potential [65], whereas standard united atom OPLS parameters were used to model methane and DCE [66]. All bond lengths and bond angles were kept fixed in the simulations, while torsional flexibility of the DCE molecule around its C-C bond was allowed. The interaction and geometry parameters of the potential models used are summarized in tables 1 and 2, respectively. The methane molecule as well as the CH_2 groups of the DCE molecules were treated as united atoms. The total potential energy of the system was assumed to be the sum of the interaction energies of all molecule pairs. The interaction energy between two molecules was expressed as the sum of Lennard-Jones and Coulomb terms acting between the interaction sites and their partial charges. Bond lengths and angles of the DCE and water molecules were kept rigid by means of the LINCS [67] and SETTLE [68] algorithms, respectively. The pairwise interactions were calculated explicitly within a centre-centre cut-off distance of 9.0 Å. Beyond this distance, Lennard-Jones contributions were truncated to zero, whereas the long range part of the electrostatic interactions was accounted for using the Particle Mesh Ewald (PME) method [69]. The temperature of the system was kept constant using the Nosé-Hoover thermostat [70,71]. The equations of motion were solved using the integration time step of 1 fs.

The system was prepared analogously to what has been described in our previous paper on chloride ion transfer [44]. A randomly chosen water molecule in the bulk aqueous phase of the pre-equilibrated penetrant-free water-DCE biphasic system [72] was replaced by one methane molecule. The energy of the resulting system was then minimized by the steepest descent method in 500000 steps, after which it was equilibrated in the (*N*,*V*,*T*) ensemble for 1 ns. The sample configurations with the methane molecule at different positions along the interface normal axis were obtained by performing a set of simulations with the *X* coordinate of the penetrant constrained at a set of different values, separated from each other by 1 Å, such that the constrained positions modelled a quasi-equilibrium path between the bulk aqueous and the bulk organic phase. Instantaneous

snapshots of the system simulated, corresponding to different positions of the methane molecule along the interface normal axis, are shown in Figure 1.

2.2. ITIM analysis and solvation free energy calculation

The profile of the solvation Helmholtz free energy, *A*, of the methane molecule was reconstructed by constrained molecular dynamics [16,17], combined with the ITIM intrinsic surface analysis method [59], as it has been described in detail in our previous paper [44]. Thus, in every simulation in which the *X* coordinate of the methane molecule was fixed, the force required to enforce this constraint was recorded at every time step. The ITIM analysis was also performed for every saved frame, in its altered formulation [44], i.e., only along a 5 × 5 quadratic grid of test lines lying close to the penetrant in the interfacial plane *YZ*, to yield the 5-6 closest interfacial molecules. This grid was determined on the fly for each configuration. The spacing of the test lines was 0.5 Å, whereas the radius of the probe sphere was set to 1.25 Å, in accordance with the recommendations of Jorge et al. [63]. The *X* position of the intrinsic surface at the *YZ* point of the penetrant was determined by the triangular interpolation method [52]. Knowing the position of the interface and of the penetrant, the (signed) intrinsic distance between them, d_{intr}, was calculated for every saved configuration and matched with the relevant instantaneous value of the constraining force. Finally, the instantaneous force vs. intrinsic distance function was integrated according to the algorithm described in full detail in our previous paper [44].

3. Results and discussion

The non-intrinsic solvation free energy profile of methane across the water-1,2-DCE interface, together with the global mass density profile of the aqueous and organic phases, are plotted in Figure 2, whereas the corresponding intrinsic free energy profile, calculated according to the protocol described in [44], is shown in Figure 3. It should be noted that direct comparison of these profiles is not a trivial task, since the non-intrinsic profile is obtained as a function of the penetrant position along the macroscopic interface normal axis, *X*, whereas the independent variable of the intrinsic profile is the signed distance of the penetrant from the intrinsic water surface, d_{intr}, the value of which is negative in the aqueous and positive in the apolar phase. A direct correspondence between the two independent variables is not possible, but a comparison of the qualitative features of the two profiles can be carried out.

It is clearly seen from the negative slope of the free energy profiles that the system favours

configurations in which the apolar methane molecule is found in the medium of smaller dielectric constant, which is 1,2-dichloroethane in our case. The solvation free energy difference of methane in the two phases turns out to be about 59 kJ/mol from both profiles, with the difference between the intrinsic and non-intrinsic PMFs being less than the value of $k_B T$ at 298 K. This good agreement is expected, since the intrinsic vs. non-intrinsic treatment of the interface should not affect bulk phase properties, such as the solvation free energy of the solute in the two bulk liquids. Interestingly, the magnitude (but, obviously, not the sign) of this solvation free energy difference is close to what has been calculated previously for different ions in the same system, i.e., about -75 kJ/mol for SCN^- [42] and -55 kJ/mol for Cl^- [44]. This similarity originates from the fact [73] that ions are transferred to the organic phase together with the water molecules constituting their first solvation shell [42,44], and hence the unfavourable case (i.e., methane in water, and hydrated ions in DCE) involves water-apolar contacts in both cases. The energy cost corresponding to these unfavourable contacts should primarily depend on the number of such contacts, i.e., the number of water molecules constituting the first hydration shell of the penetrant (as in the case of methane in water these molecules are in contact with the apolar methane molecule, whereas in the case of the hydrated chloride ion in DCE these waters are in contact with the surrounding DCE molecules). Since the Cl^- ion and methane molecule are roughly of the same size (their Lennard-Jones distance parameter σ being 3.55 and 3.73 Å, respectively [66]), it is not surprising that their hydration shells are roughly the same size, leading to solvation free energy differences of similar magnitude in the two phases. Consistently, this difference is about 30% higher in the case of the larger SCN^- ion, the hydration shell of which consists of more water molecules.

It is quite instructive to compare the obtained intrinsic PMF of methane with that of the chloride ion in the same interfacial system [44]. This latter profile is shown in the inset of Fig. 3. Comparing the two profiles one can observe three main points of difference. First and most obviously, the slopes of the two profiles have opposite sign, which is due to the fact that the solubility of the chloride ion in water is higher than that in DCE, whereas the solubility of methane shows the opposite trend.

The second difference is the absence/presence of a local maximum for situations in which the penetrant is found at the phase boundary. As it has been shown previously [44], in the case of the chloride ion the local maximum is present for the following reason. Upon crossing the interface from the aqueous to the apolar phase the ion pulls out a water “finger” and remains at its tip until the first hydration shell is fully detached from the water surface. After this detachment the first hydration shell of the ion is fully recovered, and hence becomes more compact (i.e., having less

contact with the apolar phase) than before the detachment, when it adopted the shape of an elongated “finger”. Furthermore, since the ion is located at the tip of this finger, it is in direct contact with the DCE molecules before the detachment, but little such contact exists after the detachment, when the hydrated ion is fully surrounded by the apolar phase. In the case of the methane molecule, however, no such pronounced maximum is visible. The fluctuations observed in this region are much smaller than the value of $k_B T$, being in the order of magnitude of the statistical error. This finding implies that the first solvation shell of methane is not extracted to the opposite phase in either direction. Formation of a water finger and co-extraction of the first hydration shell is not expected for apolar penetrants. To confirm this finding we calculated the methane-water pair correlation function and, indeed, we did not find any water molecules in contact with the methane penetrant when the methane molecule was already in the apolar phase. Further, the monotonic nature of the obtained profile also reveals that no such phenomena occurs even in the opposite situation, i.e., no DCE finger is formed when the penetrant is close to the interface at its organic side (see the snapshots in Fig. 1).

The third difference is the absence/presence of an under-sampled region, which is clearly visible in the profile of the chloride ion but does not appear in the profile of methane. This difference can again be attributed to the fact that methane, unlike the chloride ion, is extracted to the organic phase without its hydration shell. The presence of such a “gap” in the chloride profile near the interface indicates that certain positions along the interface normal axis, which are situated very close to the intrinsic surface at the organic side, are visited by the penetrant with almost zero probability. The physical picture behind this effect is the instantaneous withdrawal of the aqueous phase to its original position after the final detachment of the hydrated ion. Indeed, before the hydrated ion is detached from the aqueous surface the chloride ion is at the aqueous side of the intrinsic interface. However, after the final detachment the centre-of-mass of the ion has to be farther away from the interface, at the organic side, than the radius of the hydrated ion. An apolar particle that does not bring any water molecules with itself, can, on the other hand, pass the interface smoothly, visiting all values of the reaction coordinate (i.e.: the intrinsic distance from the water surface) with a finite, non-zero probability.

4. Summary and conclusions

In this paper we have presented the calculation and analysis of the intrinsic solvation free energy profile of methane through the liquid-liquid interface of water and 1,2-dichloroethane. The free energy profiles and the hydration properties of the penetrant have been analyzed. The free energy difference between the two phases has turned out to be around 59 kJ/mol both by the intrinsic and non-intrinsic approach. This value is relatively large, its magnitude being in the same order of magnitude (but having the opposite sign) as those obtained previously for the Cl^- [44] and SCN^- ions [44].

The features of the intrinsic free energy profile of methane, as compared to that of the chloride ion, indicate a much smoother transfer, and can be summarized in three main points. First of all, the slope of the two profiles has an opposite sign as a result of the substantial difference in the solubilities of the two species in the aqueous and organic medium. Secondly, no pronounced local maximum is seen in the profile of methane, which is due to the fact that, contrary to the chloride ion, it does not pull either a water finger out of the aqueous, or a DCE finger out of the organic phase. The third main difference is the lack of an under-sampled region in the profile of methane, which is the consequence of the fact that, unlike in the case of the chloride ion, methane is transported to the apolar phase without its first hydration shell.

Acknowledgements

This project is supported by the Hungarian OTKA Foundation under project No. 104234.

References

[1] F. Franks, S. Mathias (Eds.), Biophysics of Water, Wiley, New York, 1982.

[2] B. H. Honig, W. L. Hubbell, R. F. Flewelling, Annu Rev. Biophys. Biophys. Chem. 15 (1986) 163.

[3] S. McLaughlin, Annu Rev. Biophys. Biophys. Chem. 18 (1989) 113.

[4] H. H. Girault, D. J., Schiffrin, in: A. J. Bard (Ed.), Electroanalytical Chemistry, Dekker, New York, 1989.

[5] C. M. Starks, C. L. Liotta, M. Halpern, Phase Transfer Catalysis, Chapman & Hall, New York, 1994.

[6] R. E. Panzer, M. G. Schaer, J. Electrochem. Soc. 112 (1965) 1136.

[7] B. G. Cox, A. J. Parker, *J. Am. Chem. Soc.* 95 (1973) 40.

[8] R. Smits, D. L. Massart, Electrohim. Acta 21 (1976) 431.

[9] R. Fuchs, W. K. Stephenson, Canadian J. Chem. 63 (1985) 349.

[10] J. V. Coe, Chem. Phys. Lett. 229 (1994) 161.

[11] S. Dumont, W. Cheng, V. Serebrov, R. K. Beran, I. Tinoco Jr, A. M. Pyle, C. Bustamante, Nature 439 (2006) 105.

[12] G. M. Torrie, J. P. Valleau, J. Comput. Phys. 23 (1977) 187.

[13] M. Mezei, J. Comput. Phys. 68 (1987) 237.

[14] S. Izrailev, S. Stepaniants, B. Isralewitz, D. Kosztin, H. Lu, F. Molnar, W. Wriggers, K. Schulten, in: P. Deuflhard, J. Hermans, B. Leimkuhler, A. Mark, R. Skeel, S. Reich (Eds.), Computational Molecular Dynamics: Challenges, Methods, Ideas, Springer, Berlin, 1999, pp. 39-65.

[15] A. Laio, M. Parinello, Proc. Natl. Acad. Sci. USA 99 (2002) 12562.

[16] T. Mülders, P. Krüger, W. Swegat, J. Schlitter, J. Chem. Phys. 104 (1996) 4869.

[17] M. Sprik, G. Ciccotti, J. Chem. Phys. 109 (1998) 7737.

[18] B. Widom, J. Chem. Phys. 39 (1963) 2808.

[19] P. Jedlovszky, M. Mezei, J. Am. Chem. Soc. 122 (2000) 5125.

[20] S. J. Marrink, H. J. C. Berendsen, J. Phys. Chem. 98 (1994) 4155.

[21] S. J. Marrink, H. J. C. Berendsen, J. Phys. Chem. 100 (1996) 16729.

[22] I. Benjamin, J. Chem. Phys. 110 (1999) 8070.

[23] P. Jedlovszky, M. Mezei, J. Phys. Chem. B 107 (2003) 5322.

[24] W. Shinoda, M. Mikami, T. Baba, M. Hato, J. Phys. Chem. B 108 (2004) 9346.

[25] S. Paul, A. Chandra, Chem. Phys. Lett. 400 (2004) 515.

[26] L. B. Pártay, P. Jedlovszky, P. N. M. hoang, S. Picaud, M. Mezei, J. Phys. Chem. C 111 (2007) 9407.

[27] C. D. Wick, T. M. Chang, L. X. Dang, J. Phys. Chem. B 114 (2010) 14965.

[28] A. K. Shaytan, V. A. Ivanov, K. V. Shaitan, A. R. Khokhlov, J. Comp. Chem. 31 (2010) 204.

[29] I. Benjamin, J. Chem. Phys. 95 (1991) 3698.

[30] I. Benjamin, Science 261 (1993) 1558.

[31] K. Schweighoffer, I. Benjamin, J. Phys. Chem. 99 (1995) 9974.

[32] L.Lauterbach, E. Engler, N. Muzet, L. Troxler, G. Wippf, J. Phys.Chem. B 102 (1998) 245.

[33] L. X. Dang, J. Phys.Chem. B 103 (1999) 8195.

[34] P. A. Fernandes, M. N. D. S.Cordeiro, J. A. N. F. Gomes, J. Phys. Chem. B 103 (1999) 8930.

[35] P. A. Fernandes, M. N. D. S.Cordeiro, J. A. N. F. Gomes, J. Phys.Chem. B 104 (2000) 2278.

[36] L. X. Dang, J. Phys.Chem. B 106 (2002) 10388.

[37] A. Grossfield, P. Y. Ren, J. W. Ponder, J. Am. Chem. Soc. 125 (2003) 15671.

[38] P. B. Petersen, R. J. Saykally, M. Mucha, P. Jungwirth, J. Phys. Chem. B. 109 (2005) 10915.

[39] P. Jungwirth, D. *J.* Tobias, *Chem. Rev.* 106 (2006) 1259.

[40] L. M. Pegram, M. Thomas Record, Proc. Natl. Acad. Sci. 103 (2006) 14278.

[41] C. D. Wick, L. X. Dang, J. Phys. Chem. C 112 (2008) 647.

[42] M. Darvas, M. Jorge, M. N. D. S. Cordeiro, P. Jedlovszky, J. Phys. Chem. C 115 (2011) 11140.

[43] D. Boda, J. Giri, D. Henderson, B. Eisenberg, D. Gillespie, J. Chem. Phys. 134 (2011) 055102.

[44] M. Darvas, M. Jorge, M. N. D. S. Cordeiro, M. Sega, S. S. Kantorovich, P. Jedlovszky, J. Phys. Chem. C, submitted.

[45] J. S. Rowlinson, B. Widom, Molecular Theory of Capillarity, Clarendon Press, Oxford, 1982.

[46] E. Chacón, P. Tarazona, Phys. Rev. Lett. 91 (2003) 166103.

[47] E. Chacón, P. Tarazona, J. Alejandre, J. Chem. Phys. 125 (2006) 014709.

[48] J. Chowdhary, B. M. Ladanyi, J. Phys. Chem. B 110 (2006) 15442.

[49] M. Jorge, M. N. D. S. Cordeiro, J. Phys. Chem. C 111 (2007) 17612.

[50] M. Jorge, M. N. D. S. Cordeiro, J. Phys. Chem. C 1112 (2008) 2415.

[51] F. Bresme, E. Chacón, P. Tarazona, Phys. Chem. Chem. Phys. 10 (2008) 4704.

[52] M. Jorge, G. Hantal, P. Jedlovszky, M. N. D. S. Cordeiro, J. Phys. Chem. C 114 (2010) 18656.

[53] F. H. Stillinger, *J. Chem. Phys*. **76** (1982) 1087.

[54] P. Linse, J. Chem. Phys. 86 (1987) 4177.

[55] I. Benjamin, J. Chem. Phys. 97 (1992) 1432.

[56] K. Schweighoffer, I. Benjamin, J. Phys. Chem. 99 (1995) 9974.

[57] P. A. Fernandes, M. N. D. S. Cordeiro, J. A. N. F. Gomes, J. Phys. Chem. B 103 (1999) 6290.

[58] D. Michael, I. Benjamin, J. Chem. Phys. 114 (2001) 2817.

[59] L. B. Pártay, G. Hantal, P. Jedlovszky, Á. Vincze, G. Horvai, J. Comp. Chem. 29 (2008) 945.

[60] M. Mezei, J. Mol. Graphics Modell. 21 (2003) 463.

[61] A. P. Wilard, D. Chandler, J. Phys. Chem. B 114 (2010) 1954.

[62] M. Sega, S. S. Kantorovich, P. Jedlovszky M. Jorge, J. Chem. Phys., 138 (2013) 044110.

[63] M. Jorge, P. Jedlovszky, M. N. D. S. Cordeiro, J. Phys. Chem. C 114 (2010) 11169.

[64] E. Lindahl, B. Hess, D. van der Spoel, J. Mol. Mod. 7 (2001) 306.

[65] W. L. Jorgensen, J. Chandrashekar, J. D. Madura, R. Impey and M. L. Klein, J. Chem. Phys. 79 (1983) 926.

[66] W. L. Jorgensen, J. Tirado-Rives, J. Am. Chem. Soc. 110 (1988) 1657.

[67] B. Hess, H. Bekker, H. J. C. Berendsen, J. G. E. M. Fraaije, J. Comp. Chem. 18 (1997) 1463.

[68] S. Miyamoto, P. A. Kollman, J. Comp. Chem. 13 (1992) 952.

[69] U. Essman, L. Perera, M. L. Berkowitz, T. Darden, H. Lee, L. G. Pedersen, J. Chem. Phys. 103 (1995) 8577.

[70] S. Nosé, Mol. Phys. 52 (1984) 255.

[71] W. G. Hoover, Phys. Rev. A 31 (1985) 1695.

[72] G. Hantal, M. Darvas, L. B. Pártay, G. Horvai, P. Jedlovszky, J. Phys.: Condens. Matter 22 (2010) 284112.

[73] T. Osakai, A. Ogata, K. Ebina, J. Phys.Chem. B 101 (1997) 8341.

Tables

Table 1. Potential parameters of the water, DCE, and methane molecules.

Molecule	Interaction site	σ / Å	ε / kJ mol^{-1}	q / e
Water[a]	O_w	3.154	0.649	0.000
	H_w	0.000	0.000	0.520
	M_w[b]	0.000	0.000	-1.040
CH_4[c]	CH_4	3.730	1.229	0.000
DCE[c]	CH_2	3.800	0.494	0.227
	Cl	3.400	1.255	-0.227

[a]TIP4P model, ref. [65].
[b]Non-atomic interaction site, placed along the H-O-H bisector 0.15 Å away from the O atom toward the hydrogens.
[c]Lennard-Jones parameters correspond to the OPLS model, ref. [66], fractional charges are taken from ref. [55].

Table 2: Geometry parameters of the molecular models used in the simulations

Molecule	Bond	Length (Å)	Bond angle	Angle (deg)
Water	O-H	0.9572	H-O-H	104.52
DCE	CH_2-CH_2	1.53	Cl-CH_2-CH_2	108.2
	CH_2-Cl	1.79		

Figure captions

Fig. 1. Instantaneous snapshots of the water/1,2-DCE interfacial system with the methane molecule being at different distances from the intrinsic interface, i.e., in the bulk aqueous phase (d_{intr} = -5.0 Å, top panel), right at the interface (d_{intr} = 0.3 Å, middle panel) and in the bulk DCE phase (d_{intr} = 6.1 Å, bottom panel). Water and DCE molecules are represented by blue and grey rods respectively, while the united atom methane molecule is shown as a purple sphere.

Fig. 2. Non-intrinsic solvation Helmholtz free energy profile of methane (bottom panel), shown together with the global mass density profiles (top panel) of the aqueous (filled circles) and the DCE (open circles) phases. The dashed vertical line indicates the position of the Gibbs dividing surface (GDS).

Fig. 3. Intrinsic solvation Helmholtz free energy profile of methane across the water–DCE liquid-liquid interface. The inset shows the same profile obtained previously for the chloride ion [44].

Figure 1.

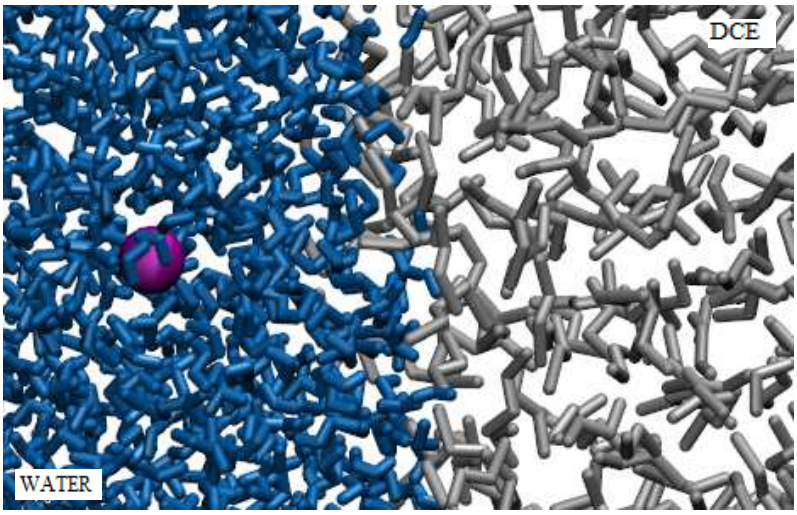

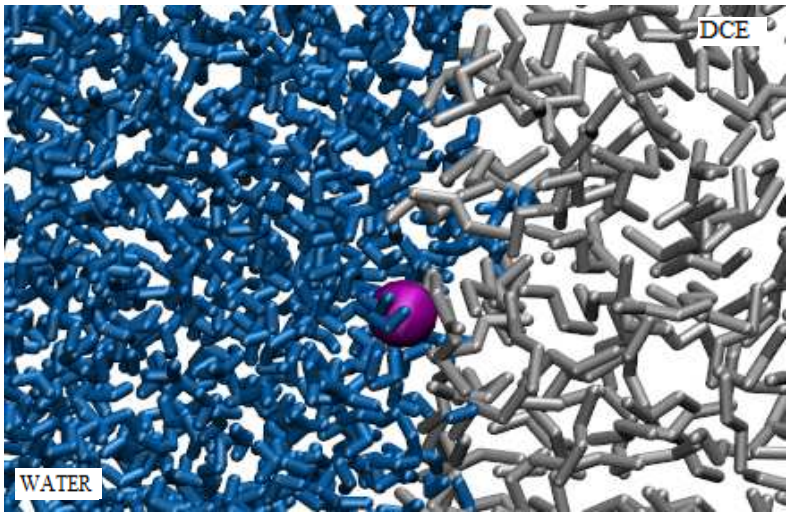

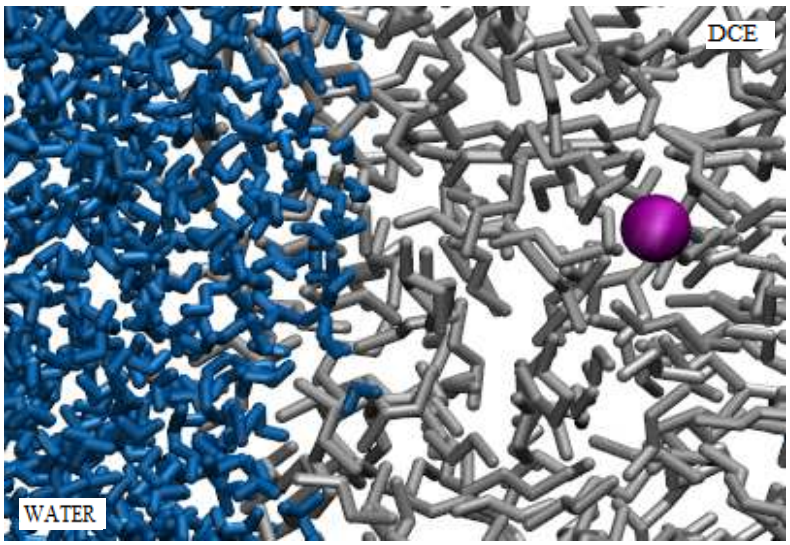

Figure 2.

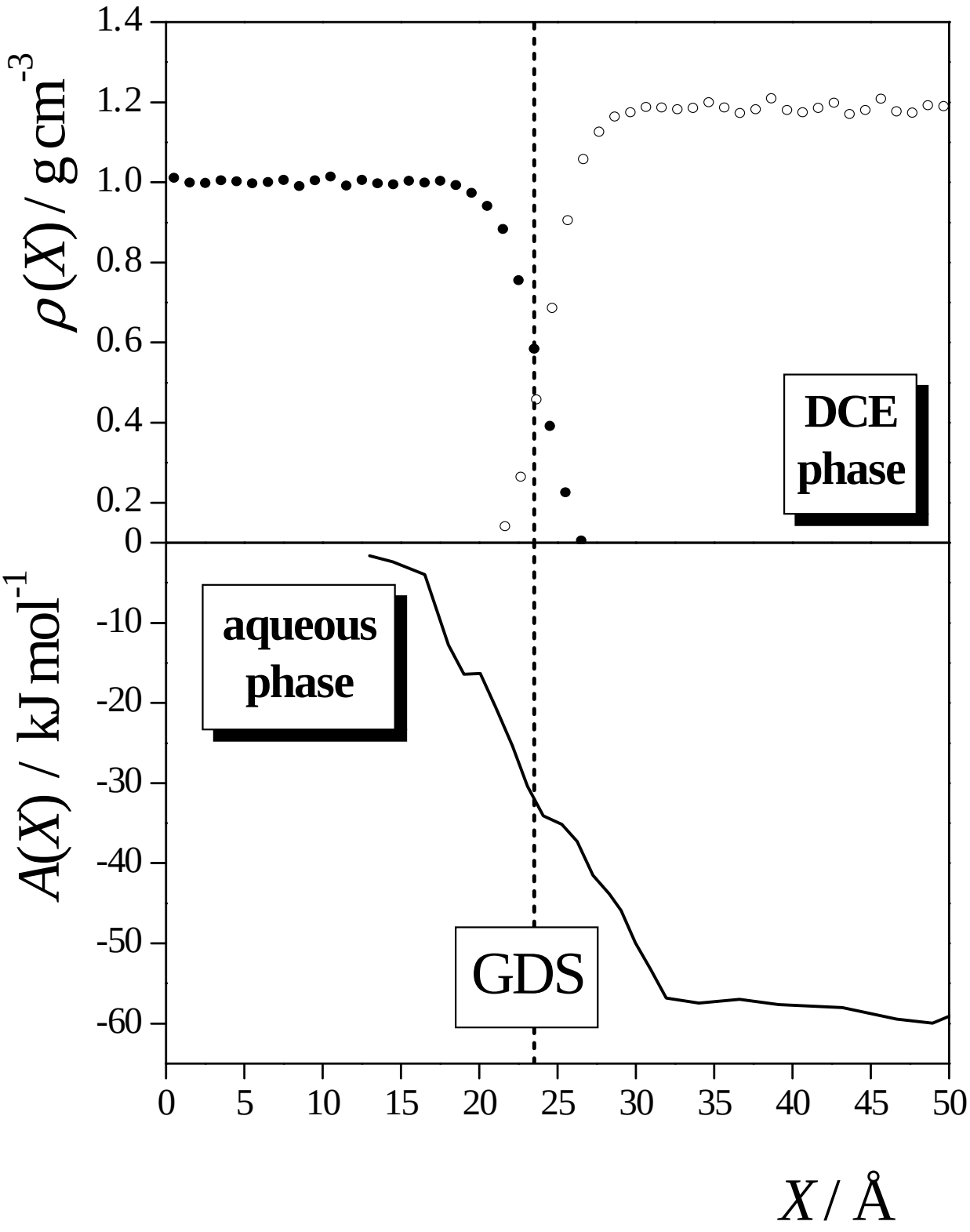
1.4
1.2
1.0
0.8
0.6
0.4
0.2
0
ρ(X) / g cm-3
DCE
phase
aqueous
phase
-10
-20
-30
-40
-50
-60
A(X) / kJ mol-1
GDS
0
5
10
15
20
25
30
35
40
45
50
X / Å

Figure 3.